

Macromolecules

Volume 28, Number 6

March 13, 1995

© Copyright 1995 by the American Chemical Society

Studies on Conducting Polymers. 1. Aniline-Initiated Polymerization of Nitroanilines

Bidhan C. Roy, Maya Dutta Gupta, and Jayanta K. Ray*

Department of Chemistry, Indian Institute of Technology, Kharagpur 721302, India

Received March 9, 1994; Revised Manuscript Received September 16, 1994*

ABSTRACT: The synthesis of homopolymers based on *m*-nitroaniline and *p*-nitroaniline by aniline-initiated ammonium peroxydisulfate oxidation, has been attempted. Poly(*m*-nitroaniline) and poly(*p*-nitroaniline), thus synthesized, were characterized by infrared spectroscopy (IR), ultraviolet–visible absorption spectroscopy (UV–vis), ^1H nuclear magnetic resonance spectroscopy (^1H -NMR), X-ray photoelectron spectroscopy (XPS), X-ray diffraction (XRD), and thermal analysis (TG-DTA). The XPS results indicate chemical shifts of different environments for the N 1s, corresponding to the amino and nitro groups. Room temperature conductivities of the HCl-doped homopolymers are very low compared to polyaniline and are of the order of $10^{-6} \text{ S cm}^{-1}$. An attempt has been made to rationalize the results on the basis of the effect of $-\text{NO}_2$ substituents on the polymer structure.

Introduction

The synthesis and development of conducting polymers with the potential of replacing the expensive and rapidly depleting “metal” reserves have been one of the marvels of synthetic organic chemistry.^{1–3} Among the organic conducting polymers, polyaniline is unique, with the typical chemical and mechanical properties of a polymer along with the major electronic characteristics of metals as well as semiconductors,^{4–6} being at the same time relatively inexpensive and stable under ambient conditions,^{3,7} with readily available simple procedures of synthesis. These polymers are widely employed in the fabrication of modified electrodes and sensors, secondary batteries, electrochromic materials and microelectronic devices.^{3–6} The ring-substituted polyanilines with lower conductivities in the semiconducting range also find high technology applications in their use as antistatic and EMI shielding materials.

Examination of reported data indicate that substituent groups may markedly affect the polymerizability of anilines, with the strongly electron withdrawing substituents like the $-\text{NO}_2$ group retarding the polymerization.^{8–12} As the k_b (basicity constant) values of the three mononitroanilines are different from each other, *m*-nitroaniline > *p*-nitroaniline >>> *o*-nitroaniline, the ease of polymerization of these may differ significantly, since the relative k_b values may be taken as the measure of electron-withdrawing capacity by the nitro group in the respective positions. In the present work an at-

tempt has been made to synthesize poly(nitroanilines), with the nitro substituent group in different positions, in order to elucidate the structure–property relations that govern the polymerization capacity and other physico-chemical characteristics of substituted polyanilines.

Experimental Section

Materials and Instrumentation. Aniline, *m,p*-nitroaniline were purchased from S.D. Chemical. Aniline was doubly distilled prior to polymerization, and nitroanilines were recrystallized in suitable solvent. Ammonium peroxydisulfate, purchased from S.D. Chemical, was used as the oxidant in polymerization. All aqueous solutions were prepared in distilled water. Elemental analysis was performed by using a Heraeus, Carlo Erba 1108 C, H, N elemental analyzer. Intrinsic viscosities were determined in 96% sulfuric acid at 30 °C using polymer concentrations between 0.07 and 0.4 g/dL with a Ubbelohde capillary viscometer. The IR spectra of polymers in KBr pellets were recorded on a Perkin-Elmer (Model 883) infrared spectrometer. The UV–vis spectra of very dilute solutions of polymers in DMSO were measured on a Shimadzu UV-3100 spectrometer. ^1H -NMR spectra of the polymer bases were recorded on a Bruker FACF-200 FT-NMR spectrometer operating at 200 MHz. Deuterated dimethyl sulfoxide ($\text{DMSO}-d_6$) was used as the solvent, and tetramethylsilane (TMS), as an internal standard. Dilute solutions of the polymers (0.5–1% w/v) were prepared to ensure maximum dissolution. X-ray photoelectron spectroscopic analysis was performed with VG ESCA LAB MkII spectrometer using an Al K α radiation source (1487 eV) at a base pressure of 10^{-7} Torr. All binding energies were referenced to the peak in the C 1s envelope, defined at 285.0 eV to compensate for surface charging. XRD profiles were recorded on a Philips PW-1840 X-ray diffractometer using Cu K α radiation of wavelength

* Abstract published in *Advance ACS Abstracts*, January 15, 1995.

Table 1. Experimental Details for the Polymerization of Aniline and Nitroanilines

sample (abbrev)	yield (%)	reacn temp (°C)	conductivities (S cm ⁻¹)
polyaniline (PAN-HCl)	66	0–5	10
poly(<i>p</i> -nitroaniline) (PPN-HCl)	32	30–35	5.6×10^{-6}
poly(<i>m</i> -nitroaniline) (PMN-HCl)	36	0–5	3.5×10^{-6}

0.154 nm and a continuous scan of 3° min⁻¹. The instrument was operated at 40 kV and 20 mA. Thermal analyses (TG, DTA) of the polymer powders (4 mg) were done on a Shimadzu DT-40 unit, under a dynamic dry air flow of 50 cm³ min⁻¹. A heating rate of 10 °C min⁻¹ was used. The analyses were performed from room temperature to 880 °C. Conductivity measurements were carried out by the two-probe technique using a Philips PR 9500 bridge at room temperature. Dry powdered samples were made into pellets using a steel die of 1.28 cm diameter in a hydraulic press under a pressure of 4500 kg cm⁻².

Synthesis. Polymers were prepared by ammonium peroxydisulfate oxidation in a manner similar to that of polyaniline.¹³ Pure nitroanilines do not form a homopolymer even if the reactants are kept for 48 h at room temperature with stirring. By addition, however, of a few drops of aniline (15 mol %) to the system, polymerization took place at different temperatures (Table 1). A strong electron withdrawal effect exerted by the substituent nitro group possibly inhibits the oxidation (initiation). In the presence of aniline, polymerization is no longer hampered. This kind of monomer-initiated polymerization is not known, but initiation by dimers has been reported.⁸

Nitroaniline (14.49 mmol) and aniline (15 mol % of nitroaniline) were dissolved in 150 mL of 1 M HCl. A solution of (NH₄)₂S₂O₈ (2.89 g, 12.67 mmol) in 50 mL of 1 M HCl was added dropwise with stirring over a period 30–40 min. With stirring for 2 h, at the same temperature (Table 1), the solution was further stirred for about 6 h at room temperature. The resulting brownish-black precipitate was washed with 1 M HCl until the filtrate was colorless and finally washed several times with ethanol. Under the same condition, *o*-nitroaniline could not be polymerized.

A part of the polymer was transferred into a conical flask containing 100 mL of 1 M HCl and was stirred for about 4 h at room temperature. The resulting material was filtered, and dried in a vacuum desiccator in the presence of P₂O₅ (48 h) to yield the HCl-doped polymer. Another portion of the polymer was suspended in 100 mL of 0.1 M NH₄OH solution with stirring for 6 h at room temperature and filtered. This residue was dried in a vacuum desiccator for 48 h in presence of P₂O₅. The HCl-doped polymer was thus converted into the free base. Table 1 summarizes results of the polymer preparations. The elemental analysis gave; C, 55.89 (calc for C₂₄H₁₄N₂O₈, 56.47); H, 3.32 (2.74); N, 19.69 (21.96) for poly(*p*-nitroaniline); C, 56.50 (56.47); H, 3.26 (2.74); N, 19.61 (21.96) for poly(*m*-nitroaniline). The general structures of poly(*p*-nitroaniline)/(PPN) and poly-

Table 2. Solubility and Viscosity of the Polymers^a

solvent	PMN	<i>n</i> _{int} (dL/g) at 30 °C	PPN	<i>n</i> _{int} (dL/g) at 30 °C
H ₂ O	i		i	
benzene	i		i	
CHCl ₃	ss		ss	
C ₂ H ₅ OH	i		i	
CH ₃ CN	i		i	
HCl (conc)	i		i	
H ₂ SO ₄ (96%)	s	0.107	s	0.090
THF	ms		ms	
DMF	s		s	
DMSO	s		s	
NMP	s		s	

^a i, insoluble; ss, slightly soluble; ms, moderately soluble; s, soluble; *n*_{int}, intrinsic viscosity. Abbreviations: DMF, dimethylformamide; DMSO, dimethyl sulfoxide; NMP, *N*-methylpyrrolidone.

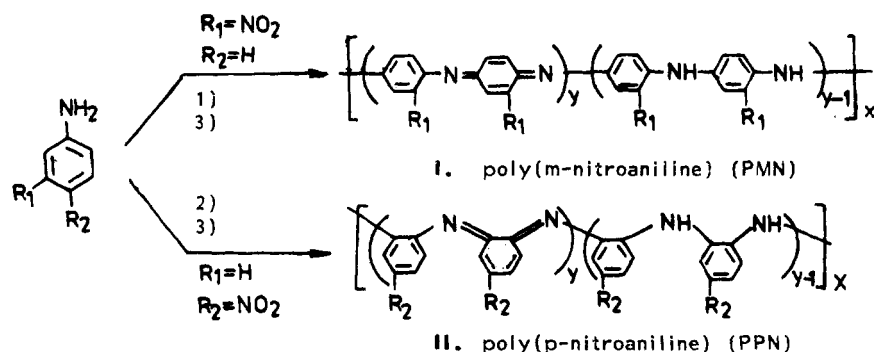
(*m*-nitroaniline/(PMN), could be represented schematically as shown in Scheme 1.

In this investigation all the experiments were performed on the base form of the polymers, except for the electrical conductivity measurements, for which the HCl-doped polymer samples were used.

Results and Discussion

The polymerization of nitroanilines by peroxydisulfate oxidation, using aniline as an initiator, was carried out at different temperatures. *m*-Nitroaniline was completely soluble in 1 M HCl at 0–5 °C, but *p*-nitroaniline was only soluble at 30 °C (Table 1). In poly(*p*-nitroaniline) (PPN) the polymerization should take place by coupling at the ortho-position to the –NH₂ group, as the para-position is already blocked by a –NO₂ group and a stable free radical should be generated at the ortho position. In *m*-nitroaniline (PMN), coupling should be more favorable at the para-position to the –NH₂ group, maintaining the head-to-tail sequence as in polyaniline, with lesser steric hindrance (Scheme 1). It also suffers less electronic deactivation effect due to the –NO₂ group, as is apparent from its relatively higher basicity. The facile polymerization (Table 1) observed in *m*-nitroaniline at lower temperatures follows as a result.

Table 2 lists the solubility characteristics of the polymers. In general, both the polymer powders were completely soluble in polar solvents such as NMP, DMSO, and DMF. These were also completely soluble in H₂SO₄ (96%), which was used for measuring the viscosities of the polymers. The viscosity data (Table 2) show qualitatively that the molecular weights of the

Scheme 1

- 1) 1M HCl and (NH₄)₂S₂O₈, at 0–5°C;
- 2) 1M HCl and (NH₄)₂S₂O₈, at 30–35°C,
- 3) 0.1M NH₄OH solution.

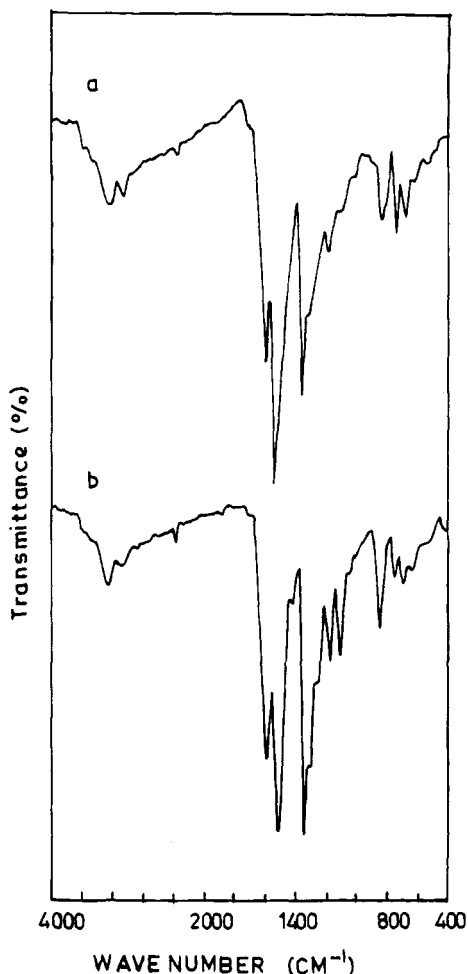


Figure 1. Infrared spectra of (a) poly(*m*-nitroaniline) and (b) poly(*p*-nitroaniline).

prepared polymers are low, since the polymer precipitates during the polymerization reaction and may not further polymerize in the solid state. Polyaniline on the other hand shows a significantly higher intrinsic viscosity ($\eta_{\text{int}} = 0.57 \text{ dL/g}$ at 30°C),¹⁴ and this is expected, as it should have a higher molecular weight, being free from the steric effects and also the deactivating influence of the substituent that retard chain growth. Viscosity data further indicate that the molecular weight of PPN may be lower than that of PMN, which suggest that steric effects preventing growth may be operative in PPN, where the coupling has to take place at the ortho position.

The representative infrared spectra of PMN-base and PPN-base are shown in Figure 1. The quinonoid and benzenoid stretchings are present at 1584 (PPN), 1586 (PMN) and 1508 (PPN), 1523 (PMN) cm^{-1} , respectively.¹¹⁻¹³ The electronic-like absorption peak of $\text{N}=\text{Q}=\text{N}$ groups (where "Q" denotes the quinonoid ring) which may be taken as a measure of the level of oxidation in polyanilines, is relatively stronger in PPN-base (Figure 1).¹⁵ The presence of 1,2,4-trisubstitution in PMN-base and PPN-base is indicated by the bands in the region $731\text{--}1108 \text{ cm}^{-1}$, ascribed to the C-H in-plane and out-of-plane bending modes.¹¹⁻¹³ The symmetric $\text{N}=\text{O}$ stretch in the PMN polymer (1347 cm^{-1}) is not shifted to lower frequency as in PPN (1335 cm^{-1}).¹⁶ This is a qualitative vindication of the head-to-tail coupling undergone by *m*-nitroaniline molecules (Scheme 1) with the $-\text{NO}_2$ group in the ortho/meta-position with respect to the $-\text{NH}_2$ groups. The relative

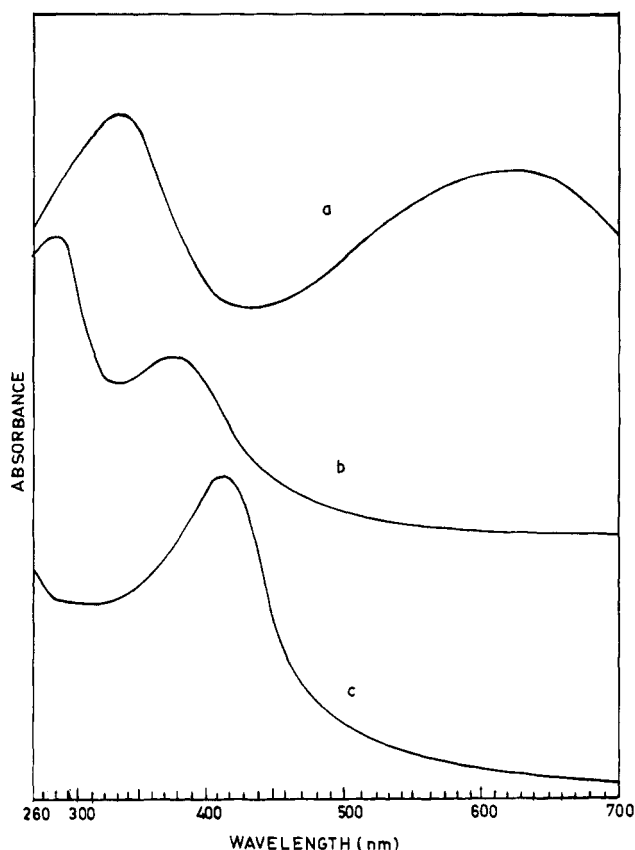


Figure 2. UV-visible absorption spectra of (a) polyaniline, (b) poly(*m*-nitroaniline), and (c) poly(*p*-nitroaniline).

intensity of the benzenoid to quinonoid absorption peaks cannot be used here as an index of oxidation, on account of the difference in the position of the asymmetric $\text{N}=\text{O}$ stretch in the PMN and PPN polymers in this region and their possible overlap with other peaks.

The UV spectrum of PAN-base in Figure 2a shows both the major absorption peaks at 322 and 624 nm, as reported earlier.⁹⁻¹³ The 322 nm peak (K-band) assigned to the $\pi\text{--}\pi^*$ transition is related to the extent of conjugation between adjacent phenyl rings in the polymer chain,¹⁷ whereas the one at 624 nm (B-band) is a measure of extended conjugation, corresponding to the "exciton" transition caused by interchain or intrachain charge transfer.¹⁸ The UV spectrum of PMN-base in Figure 2b shows both the major absorption peaks at 284 (K-band) and 373 nm (B-band). The PPN-base, however, exhibits only one band at 406 nm, as shown in Figure 2c, which thus cannot be taken as conclusive. It is expected to show a lower energy $\pi\text{--}\pi^*$ transition relative to PMN and also PAN due to a pronounced "complementary substitution" effect¹⁶ with the $-\text{NO}_2$ and $-\text{NH}_2$ groups para to each other. The blue shifts in both the absorption bands of PMN-base compared to PAN-base could be due to the steric strain caused by the $-\text{NO}_2$ group in the ortho-position to the $-\text{NH}_2$ group in the polymer chain.¹²

$^1\text{H-NMR}$ spectra of PMN-base and PPN-base are shown in Figure 3. PAN-base shows a multiplet peak at $6.6\text{--}7.4 \text{ ppm}$, which has been assigned to aromatic¹⁹ and amine protons.²⁰ The signals for PMN and PPN-base in the region $7.5\text{--}8.6 \text{ ppm}$ are assigned to the aromatic protons, and those in the region $9.2\text{--}9.6 \text{ ppm}$, to the amine protons. These two polymers show higher chemical shifts in the aromatic region in accordance with the deshielding of aromatic protons by the strong electron-withdrawing effect of the $-\text{NO}_2$ group.

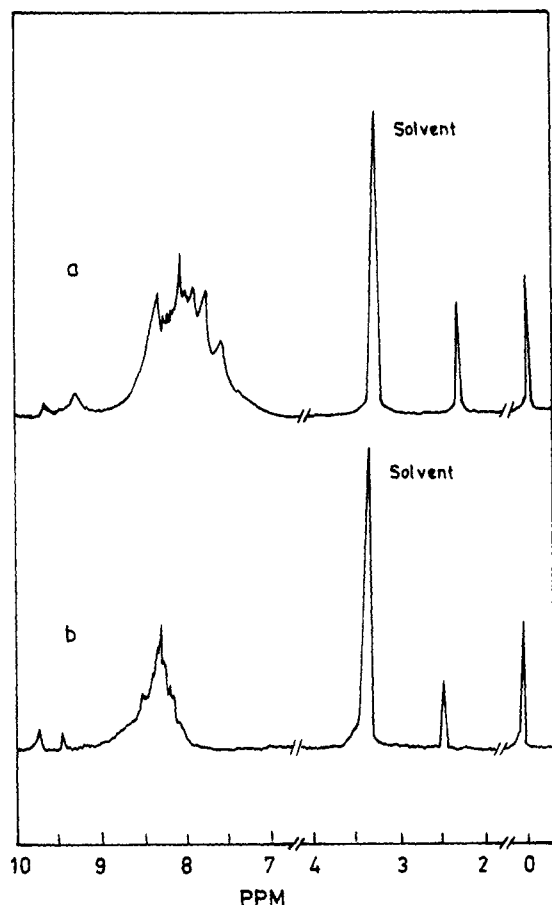


Figure 3. ^1H -NMR spectra of (a) PMN-base and (b) PPN-base in $\text{DMSO}-d_6$.

XPS core level spectra for C 1s, O 1s, and N 1s of the PMN and PPN polymers are shown in Figures 4–6 respectively. The corresponding binding energy values are given in Table 3. These are in good agreement with those previously reported.^{11,12} The N 1s spectra of both PMN and PPN consist of twin peaks, due to the separation of the amine nitrogen peak from the nitrogen of the nitro group. This is in agreement with the reported difference in chemical shifts of different environments for N 1s with the oxidized nitrogen functions like $-\text{ONO}_2$, $-\text{NO}_2$, and $-\text{ONO}$ having much higher N 1s binding energies.²¹ There are two distinct ranges of binding energies in the N 1s spectra. The amine nitrogen is in the range 399–401 eV, and the nitrogen of the nitro groups gets registered in the 404–408 eV range. The higher binding energy of the N 1s component peaks in the XPS spectrum of the PPN polymer (Figure 5) indicates that some charged N 1s species (~ 402.5 eV) may be present,^{11,12} as a positive charge on the nitrogen atom leads to a higher binding energy of the core electrons.

The X-ray diffraction profiles of PAN-base, PMN-base, and PPN-base are shown in Figure 7. All these polyanilines are characterized by the broad, amorphous scattering at $2\theta \approx 25^\circ$.^{9,22} They, however, exhibit slight crystallinity and are not totally amorphous, as indicated by the presence of peaks (Figure 7) at $2\theta = 24.2, 26.6^\circ$ (PAN-base), $2\theta = 27.2, 29^\circ$ (PMN-base), and $2\theta = 26.1, 29.6^\circ$ (PPN-base). The XRD pattern further indicates that the PPN polymer is somewhat more crystalline, with peaks being sharper than that of the PMN polymer. The observed 2θ and d values are summarized in Table 4. X-ray data indicate that diffraction patterns of both PMN-base and PPN-base are compatible with

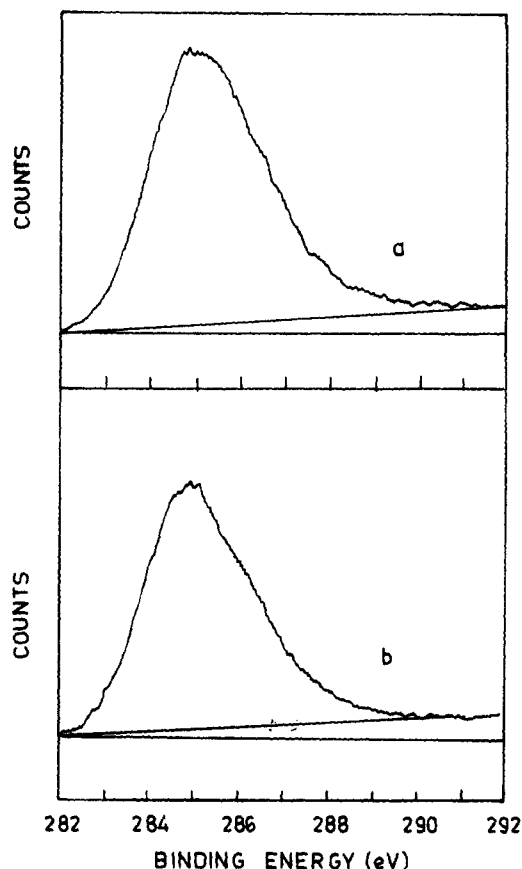


Figure 4. XPS C 1s spectra of (a) poly(*m*-nitroaniline) and (b) poly(*p*-nitroaniline).

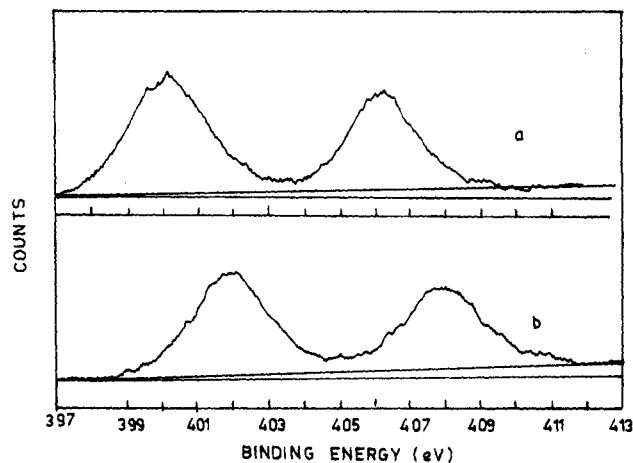


Figure 5. XPS N 1s spectra of (a) poly(*m*-nitroaniline) and (b) poly(*p*-nitroaniline).

an orthorhombic lattice. The unit cell dimensions deduced from observed 2θ and d values along with the indexed planes are given in Table 4. The unit cell parameters, a , b , and c have been defined as in earlier works.²² The increase in the unit-cell parameter a for PMN indicates a planar deformation caused by an increase in the torsional angle between the phenyl rings to relieve the steric strain due to the nitro group in the ortho-position to the amino group.⁹

Thermal analysis (TG-DTA) patterns of PMN, PPN, and PAN polymer bases in air are shown in Figures 8a, 8b, and 8c. In PMN and PPN, and also PAN, in air, the thermogram is exothermic over the entire range of analysis. Such exothermic behavior in polyanilines has been attributed to cross-linking of polymer chains and also to the rearrangement and degradation of side

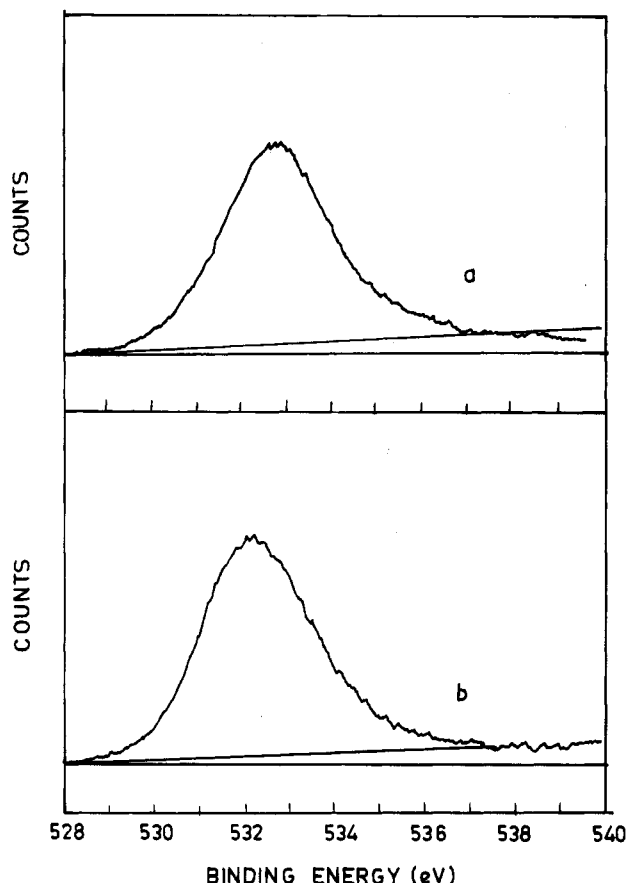


Figure 6. XPS O 1s spectra of (a) poly(*m*-nitroaniline) and (b) poly(*p*-nitroaniline).

Table 3. XPS Binding Energies for C 1s, N 1s, and O 1s Core Levels of Poly(nitroanilines)

sample	binding energy (eV)			
	C 1s	N 1s	O 1s	
PPN	285	402	407.8	532.2
PMN	285	400	406.3	532.8

Table 4. Poly(nitroaniline) Crystal Structure Parameters and 2θ values

sample	2θ (obsd) (deg)	2θ (calcd) (deg)	d value (obsd) (Å)	hkl	remark
PPN	14.65	14.69	6.04	010	orthorhombic unit cell dimensions $a = 7.03$ Å $b = 6.00$ Å $c = 11.04$ Å
	19.74	19.64	4.49	110	
	21.05	21.03	4.22	111	
	22.00	21.96	4.03	012	
	24.05	24.11	3.69	003	
	26.14	26.19	3.40	201	
	29.60	29.65	3.01	020	
	36.98	36.92	2.43	122	
	44.60	44.56	2.03	312	
PMN	10.20	10.20	8.66	100	orthorhombic unit cell dimensions $a = 8.67$ Å $b = 5.90$ Å $c = 10.65$ Å
	18.22	18.18	4.86	110	
	20.38	20.42	4.35	200	
	22.60	22.57	3.93	012	
	24.35	24.40	3.65	112	
	27.25	27.20	3.27	103	
	29.00	29.15	3.07	013	
	42.82	42.82	2.11	214	
	47.05	47.15	1.93	130	

chains.^{3,13,14} The larger mass loss suffered by PPN with 60% residual weight, compared to that of 75% in PMN (Figures 8a and 8b), prior to the final stage of decomposition, indicates an earlier onset of oxidative degradation. This may again be due to shorter chain segments in PPN polymer units. The sharp exothermic peaks

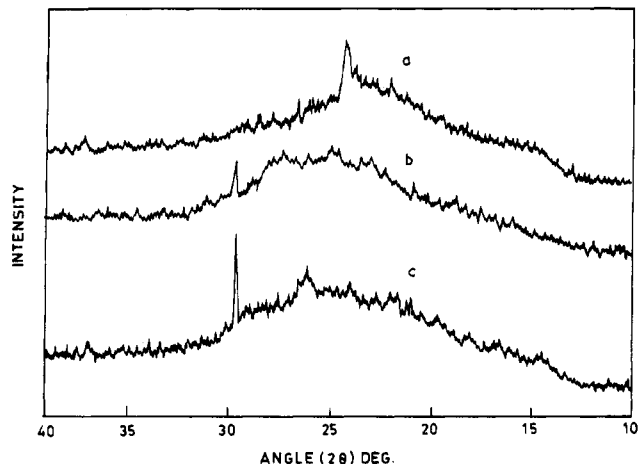


Figure 7. X-ray diffraction pattern of (a) polyaniline, (b) poly(*m*-nitroaniline), and (c) poly(*p*-nitroaniline).

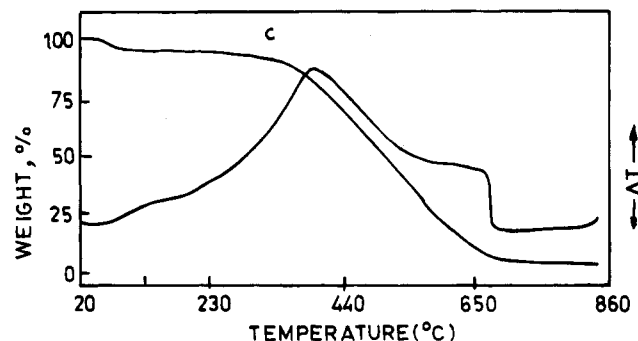
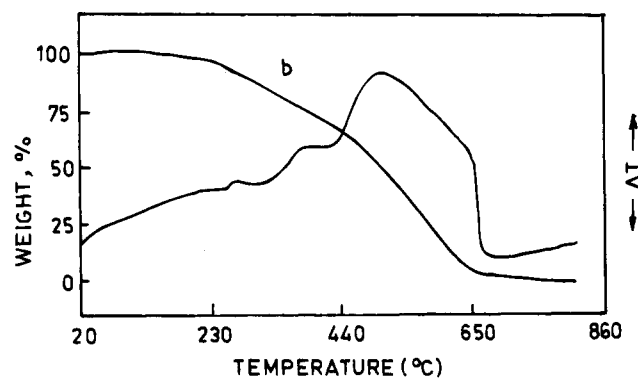
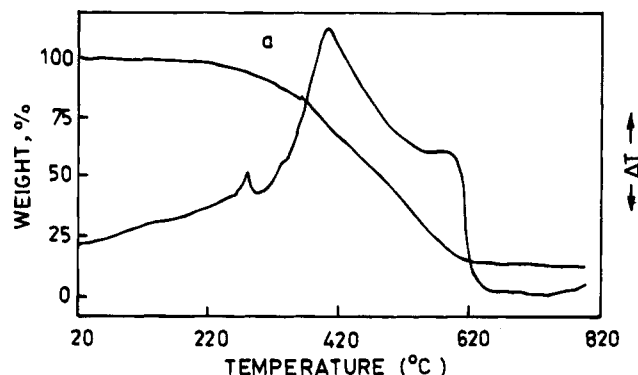


Figure 8. (a) TG-DTA thermogram of poly(*m*-nitroaniline) in air. (b) TG-DTA thermogram of poly(*p*-nitroaniline) in air. (c) TG-DTA thermogram of polyaniline.

(296 °C for PMN and 280 °C for PPN) may be due to some morphological change, possibly crystallization of the polymers. The final stage of decomposition is oxidative thermal degradation^{9,10} (Figures 8a, 8b, and 8c). The higher decomposition temperature of PPN (Table 5) may be due to the presence of cross-linked

Table 5. Thermal Degradation Parameters of Poly(nitroanilines)

sample	range of decomp temp (°C)	max decomp temp (°C)	activation energy E_a , kJ mol ⁻¹
PAN	300–620	389	18.0
PPN	427–694	513	9.3
PMN	360–630	408	11.2

products formed in the earlier stages. Thermal analysis results do not indicate any pronounced stability difference between the two nitrosubstituted polymers, though they are definitely more stable compared to PAN (Table 5), as indicated by their higher decomposition temperature. The higher stability of nitroanilines is a strong indication of intermolecular interactions induced by the nitro group. The experimental results at the present level, however, do not warrant a detailed explanation.

The room temperature conductivity measurements on HCl-doped salts of PMN and PPN polymers have been carried out, and the results are given in Table 1. Conductivities of both the substituted polymer hydrochlorides are less than that of the parent, PAN-HCl polymer by several orders of magnitude. This lowering of conductivity is in agreement with the observed conductivity pattern of substituted polyanilines.^{3,9–12} Qualitatively, in the PPN polymer the XPS measurements showing the presence of charged N 1s species and the IR spectra showing a higher level of oxidation indicate that it should have a larger conductivity. The PMN on the other hand could have increased conductivity as a result of its polyaniline type head-to-tail structural arrangement, involving less steric strain. The conductivities of the nitro-substituted polymers, however, do not show a significant difference. Apparently, reduced π -conjugation due to the steric hindrance caused in PMN by mutual ortho disposition of the $-\text{NO}_2$ and $-\text{NH}_2$ groups and that in PPN by the ortho coupling of the monomer units (Scheme 1) are possibly getting balanced, causing the leveling of conductivities.

Conclusion

Aniline-initiated polymerization of *m*- and *p*-nitroanilines, containing a strong electron-withdrawing nitro group, have been accomplished. In *m*-nitroaniline, availability of a free para-position makes polyaniline-like head-to-tail polymerization possible, whereas in *p*-nitroaniline, the para-position being blocked, ortho coupling has to take place. The resulting steric hindrance and also the electronic effect of the $-\text{NO}_2$ group possibly reduce the polymerization activity of the latter. The obtained polymers show good solubility in polar organic solvents but low intrinsic viscosities as compared to polyaniline. They exhibit characteristic ¹H NMR spectra, with both the aromatic and amine protons showing higher chemical shifts due to the deshielding effect of the nitro group. The XPS spectra indicate chemical shifts of different environments for the N 1s,

corresponding to amino and nitro groups in both the polymers. The increase in thermal stability compared to polyaniline may be due to intermolecular interactions induced by the nitro group. Lack of a significant difference in the conductivities of the two nitroaniline polymers demonstrates that steric effects operating in the respective cases play a major role, a feature that is in general agreement with reported conductivity patterns of ring-substituted polyanilines.³ Major trends observed in the IR, UV, and XRD measurements are qualitatively consistent with this conclusion.

Acknowledgment. Thanks are due to DST (New Delhi), Dr. T. B. Ghosh of the Physics Department, IIT, Kharagpur, for his help in XPS measurements, and Dr. S. Mohanty of the Chemistry Department, IIT, Kharagpur, for helping in crystal structure parameter calculations.

References and Notes

- Reynolds, J. R. *CHEMTECH*, **1988**, 18, 440.
- Naarmann, H. *Adv. Mater.* **1990**, 2, 345.
- Epstein, A. J.; MacDiarmid, A. G. *Faraday Discuss. Chem. Soc.* **1989**, 88, 317.
- Chao, S.; Wrighton, M. S. *J. Am. Chem. Soc.* **1987**, 109, 6227.
- Wei, Y.; Focke, W. W.; Wnek, G. E.; Ray, A.; MacDiarmid, A. G. *J. Phys. Chem.* **1989**, 93, 495.
- Duke, C. B.; Gibson, H. W. *Kirk-Othmer, Encyclopedia of Chemical Technology*; John Wiley & Sons, Inc.: New York, 1989; Vol. 18, p 755.
- Chan, H. S. O.; Teo, M. Y. B.; Khor, E.; Lim, C. N. *J. Therm. Anal.* **1989**, 35, 765.
- Wei, Y.; Hariharan, R.; Patel, S. A. *Macromolecules* **1990**, 23, 758.
- Gupta, M. C.; Umare, S. S. *Macromolecules* **1992**, 25, 138.
- Pandey, S. S.; Annapoorni, S.; Malhotra, B. D. *Macromolecules* **1993**, 26, 3190.
- Chan, H. S. O.; Ng, S. C.; Sim, W. S.; Seow, S. H.; Tan, K. L.; Tan, B. T. G. *Macromolecules* **1993**, 26, 144.
- Chan, H. S. O.; Ng, S. C.; Sim, W. S.; Tan, K. L.; Tan, B. T. G. *Macromolecules* **1992**, 25, 6029.
- Chiang, J. C.; MacDiarmid, A. G. *Synth. Met.* **1986**, 13, 193.
- MacDiarmid, A. G.; Chiang, J. C.; Richter, A. F.; Somasiri, N. L. D.; Epstein, A. J. *Conducting Polymers*; Alcazar Reidel Publications: Dordrecht, 1987; pp 105–120.
- Bodalia, R.; Stern, R.; Batich, C.; Duran, R. *J. Poly. Sci.* **1993**, 31, 2123.
- Chen, S. A.; Lee, H.-T. *Macromolecules* **1993**, 26, (No. 13), 3254.
- Silverstein, R. M.; Bassler, G. C.; Morrill, T. C. *Spectrometric Identification of Organic Compounds*, 4th ed.; John Wiley: Singapore, 1981; pp 127, 131, 324.
- Euler, W. B. *Solid State Commun.* **1986**, 57, 857.
- Stafstrom, S.; Bredas, J. L.; Epstein, A. J.; Woo, H. S.; Tanner, D. B.; Huang, W. S.; MacDiarmid, A. G. *Phys. Rev. Lett.* **1987**, 59, 1464.
- Kaplan, S.; Conwell, E. M.; Richter, A. F.; MacDiarmid, A. G. *J. Am. Chem. Soc.* **1988**, 110, 7647.
- Cao, Y.; Li, S.; Xue, Z.; Guo, D. *Synth. Met.* **1986**, 16, 857.
- Briggs, D. *Practical Surface Analysis by Auger and X-ray Photoelectron Spectroscopy*; John Wiley: New York, 1988; Chapter 9, pp 359–396.
- Jozefowicz, M. E.; Laversanne, R.; Javadi, H. H. S.; Epstein, A. J.; Pouget, J. P.; Tang, X.; MacDiarmid, A. G. *Phys. Rev.* **1989**, B39, 12958.

MA941252L